



Spatial and temporal variability of N₂O emissions in a subtropical forest catchment in China

J. Zhu¹, J. Mulder¹, L. P. Wu², X. X. Meng², Y. H. Wang³, and P. Dörsch¹

¹Norwegian University of Life Sciences, postbox 5003, Ås-1432, Norway

²Chongqing Academy of Environmental Sciences and Monitoring, Qi-shan Road 252, Chongqing, 401147, China

³Institute of Forest Ecology, Environment and Protection, Chinese Academy of Forestry, Wan-Shou-Shan, Beijing, 100091, China

Correspondence to: J. Zhu (jing.zhu@umb.no)

Received: 19 September 2012 – Published in Biogeosciences Discuss.: 29 October 2012

Revised: 25 January 2013 – Accepted: 4 February 2013 – Published: 1 March 2013

Abstract. Subtropical forests in southern China have received chronically large amounts of atmospheric nitrogen (N), causing N saturation. Recent studies suggest that a significant proportion of the N input is returned to the atmosphere, in part as nitrous oxide (N₂O). We measured N₂O emission fluxes by closed chamber technique throughout two years in a Masson pine-dominated headwater catchment with Acrisols (pH ~ 4) at Tieshanping (Chongqing, SW China) and assessed the spatial and temporal variability in two landscape elements typical for this region: a mesic forested hillslope (HS) and a hydrologically connected, terraced groundwater discharge zone (GDZ) in the valley bottom. High emission rates of up to 1800 µg N₂O-N m⁻² h⁻¹ were recorded on the HS shortly after rain storms during monsoonal summer, whereas emission fluxes during the dry winter season were generally low. Overall, N₂O emission was lower in GDZ than on HS, rendering the mesic HS the dominant source of N₂O in this landscape. Temporal variability of N₂O emissions on HS was largely explained by soil temperature (ST) and moisture, pointing at denitrification as a major process for N removal and N₂O production. The concentration of nitrate (NO₃⁻) in pore water on HS was high even in the rainy season, apparently never limiting denitrification and N₂O production. The concentration of NO₃⁻ decreased along the terraced GDZ, indicating efficient N removal, but with moderate N₂O-N loss. The extrapolated annual N₂O fluxes from soils on HS (0.54 and 0.43 g N₂O-N m⁻² yr⁻¹ for a year with a wet and a dry summer, respectively) are among the highest N₂O fluxes reported from subtropical forests so far. Annual N₂O-N emissions amounted to 8–10 % of the annual atmo-

genic N deposition, suggesting that forests on acid soils in southern China are an important, hitherto overlooked component of the anthropogenic N₂O budget.

1 Introduction

The global atmospheric concentration of nitrous oxide (N₂O), an important greenhouse gas and decomposer of stratospheric ozone, has increased from a pre-industrial level of 270 ppbv to 322 ppbv in 2008 (WMO, 2009). The global source strength is estimated to be 17.7 Tg N yr⁻¹, with agriculture contributing 2.8 (1.7–4.8) Tg N yr⁻¹ and soils under natural vegetation 6.6 (3.3–9.0) Tg N yr⁻¹ (IPCC, 2007; Hirsch et al., 2006). Both estimates based on bottom-up approaches (Stehfest and Bouwman, 2006) and on observations of the N₂O atmospheric column (Kort et al., 2011; D'Amelio et al., 2009; Hirsch et al., 2006) suggest that 50–64 % of the atmospheric N₂O derive from the (sub)tropical zone 0° to 30° N. Much of the N₂O attributable to this zone is emitted from forest soils (Melillo et al., 2001; Werner et al., 2007a; Rowlings et al., 2012). So far, N₂O flux data from subtropical forests are scarce making this biome an underinvestigated component of the global N₂O budget.

Large parts of southern China are situated in the humid subtropics and the dominant forest types are evergreen broadleaf and coniferous forest, many of which are found as patches in densely populated areas with intensive agriculture. Due to strong increases in the emission of nitrogen oxides (NO_x) and ammonia (NH_x), caused by combustion of fossil

fuels and massive fertilizer use, respectively (Xiong et al., 2008; Liu et al., 2011b), these forests receive high amounts of reactive nitrogen (N_r) by atmospheric deposition, mostly as ammonium (NH₄⁺). A recent study of five forested watersheds in southern China found various degrees of N saturation (Chen and Mulder, 2007a), i.e. rates of atmospheric N_r input exceeding uptake by vegetation (Aber et al., 2003) and causing elevated concentrations of nitrate (NO₃⁻) in the root zone. Larssen et al. (2011) reported moderate NO₃⁻ export with stream water in these watersheds, despite low forest productivity, suggesting major unaccounted N sinks in these ecosystems.

One possible fate of excess N may be gaseous emission as nitric oxide (NO), N₂O or dinitrogen (N₂) produced during nitrification and denitrification. Known factors controlling N₂O emissions are availability of inorganic N and degradable organic carbon (C), soil temperature, soil moisture and soil pH (Parton et al., 1996; Flessa et al., 1995; Smith et al., 2003; Weier et al., 1993; Simek and Cooper, 2002). The monsoonal climate in southern China provides favorable conditions for both nitrification and denitrification as much of the annual N input, dominated by NH₄⁺, occurs during rain storms in summer when soils are warm and N turnover rates high. Moreover, forests in southern China are often found on acidic soils. Acidity has been reported to support high N₂O/N₂ product ratios in denitrification (Liu et al., 2010b; Bergaust et al., 2010) which could result in high N₂O emissions. Acidity also inhibits autotrophic nitrification by reducing the availability of ammonia (NH₃), the actual substrate for membrane-bound ammonia mono-oxygenase in ammonia oxidizing bacteria (De Boer and Kowalchuk, 2001); on the other hand, low soil pH may enhance the apparent N₂O yield of nitrification, possibly involving chemodenitrification of nitrite (NO₂⁻) from either nitrification or dissimilatory NO₂⁻ reduction (Mørkved et al., 2007). Therefore the net effect of acidity on the production of nitrification-related N₂O is still uncertain.

Few studies have addressed N₂O emissions in Chinese subtropical forests. Tang et al. (2006) studied the temporal variation of N₂O fluxes in a pine, a mixed and an evergreen broadleaf forest on acid soils in the Dinghushan catchment, southern China throughout one year and found highest emissions during the wet-hot season. Based on weekly to biweekly measurements, they estimated an annual emission of 3.2 kg N₂O-N ha⁻¹, which is above the reported average N₂O emission of 1.2–1.4 kg N ha⁻¹ yr⁻¹ for tropical forests (Stehfest and Bouwman, 2006; Werner et al., 2007b). Fang et al. (2009) reported 2.0 to 2.4 kg N₂O-N loss ha⁻¹ yr⁻¹ based on monthly measurements along a hillslope in an evergreen broadleaf forest in the same catchment. Lin et al. (2010, 2012) estimated smaller average annual N₂O emissions of 0.13 and 0.71 kg N ha⁻¹ for pine forests in Hubei province, probably due to the higher pH of these forest soils.

Estimates of annual N₂O emissions in forested catchments are fraught by large temporal and spatial variability commonly reported for N₂O fluxes. Forests in subtropical China are typically found on sloping terrain and mountain ridges, resulting in hydrological gradients known to affect N₂O emissions. For example, Fang et al. (2009) found that N₂O emissions increased with soil moisture from hilltop to the bottom of a hillslope. Besides soil moisture, other soil factors, such as pH, texture, vegetation type and productivity may vary along hydrological flow paths, resulting in distinct spatial patterns of N₂O emissions (Osaka et al., 2006; Lark et al., 2004). Ultimately, soil factors related to topography may shape distinct nitrifier and denitrifier communities with respect to N₂O turnover (Philippot et al., 2009; Dörsch et al., 2012; Wessen et al., 2011; Banerjee and Siciliano, 2012). Thus, understanding of spatial and temporal variability of N₂O emission fluxes and their drivers on a landscape level are indispensable for improving regional estimates of N₂O emissions.

The objective of the present study was to estimate N₂O fluxes in an N-saturated forested catchment in Southwest China and to explore their main drivers in space and time. More specifically, we investigated the seasonal distribution of emission fluxes (dry versus wet season), the role of storm flow conditions on peak N₂O emissions and the spatial distribution of N₂O emissions along a hydrological flow path on a hillslope (HS) and a groundwater discharge zone (GDZ). We hypothesized that the emission strength is higher during the wet season than the dry season and that a substantial part of the annual N₂O emission occurs during transient N₂O emission peaks triggered by rain episodes. In addition, based on previous observations that the water-saturated GDZ has large N retention (Larssen et al., 2011), we hypothesized the GDZ to act as a zone of increased denitrification and hence high N₂O emission relative to the well-drained HS. Emissions of N₂O were measured together with soil parameters from summer 2009 to autumn 2010, along two transects in each of the two landscape elements, hillslope (HS) and groundwater discharge zone (GDZ). To improve flux estimates in time, a regression model is proposed interpolating temporally discrete N₂O measurements on the HS based on continuously recorded soil moisture and temperature.

2 Materials and methods

2.1 Site description

The Tieshanping (TSP) catchment is a 16.2 ha headwater catchment, 450 m a.s.l., located on a forested ridge about 25 km Northeast of Chongqing city, SW China (29°38' N 104°41' E, Fig. 1a). Details on climate, vegetation and soil characteristics as well as atmospheric N deposition can be found elsewhere (Chen and Mulder, 2007a). The area has a typical subtropical monsoonal climate with a mean

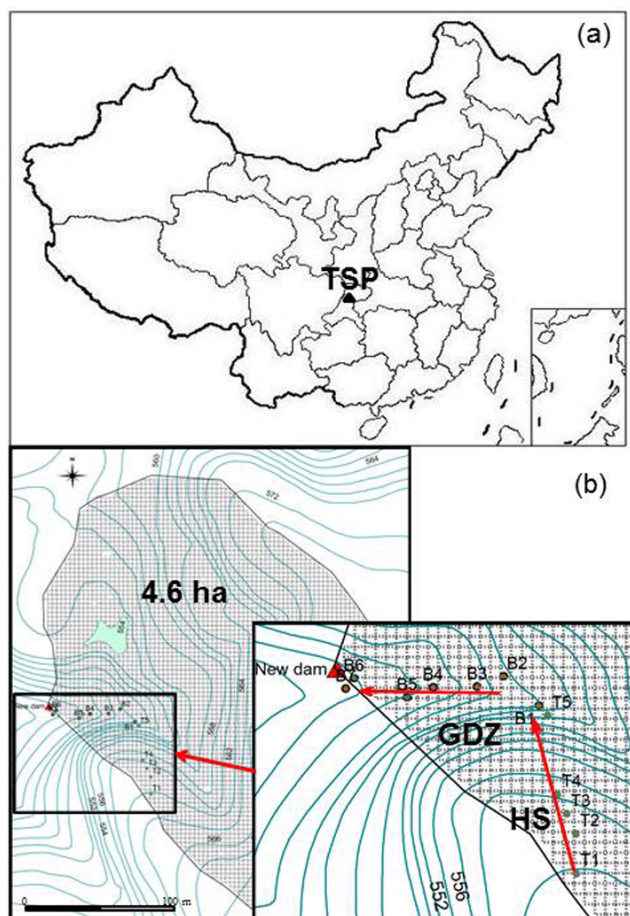


Fig. 1. (a) Location of the Tieshanping (TSP) forest catchment, Chongqing, China and (b) plot layout in the TSP catchment. Plots T1 to T5 constitute transect *T* on the hillslope (HS); plots B1 to B6 constitute transect *B* in the groundwater discharge zone (GDZ). Increasing plot numbers denote decreasing elevation along the transects. Plots T5 and B1 are at the intersection of HS and GDZ.

annual precipitation of 1028 mm and a mean annual temperature of 18.2° C (three year average, 2001–2003). Seventy-five percent (75 %) of the rainfall occurs during summer (April to September). Mean annual inorganic N deposition (from 2001–2003) was 4 g m⁻², 61 % of which occurred in the form of NH₄⁺-N (Chen and Mulder, 2007b). Data for more recent years show increasing N deposition rates to > 5 g m⁻² yr⁻¹ and confirm the relative importance of NH₄⁺ (Lei Duan, personal communication, 2011). The vegetation is a coniferous-broadleaf mixed forest dominated by Masson pine (*Pinus massoniana*) with a well-developed understory of evergreen shrubs (Chen and Mulder, 2007a). Land use is a naturally regenerated, non-managed secondary forest after the original forest was cut during 1958–1962.

For the present study, a representative 4.6 ha sub-catchment was selected, consisting of a NE facing hillslope (HS) and a hydrologically connected SE–NW oriented, terraced valley bottom acting as a groundwater discharge zone

(GDZ) (Fig. 1b). The HS is dominated by acidic, loamy yellow mountain soils (Haplic Acrisols; WRB, 2006), developed from sandstone, the predominant bedrock in the area. The soils have only a thin organic layer (O-horizon; 0–2 cm) (Table 1), likely reflecting high turnover rates of soil organic matter (SOM) in the warm and wet climate (Raich and Schlesinger, 1992; Zhou et al., 2008). Soils in the GDZ have developed from colluvium (Cambisols) and were terraced during the 1960s for vegetable cultivation but abandoned shortly after. The soils in the GDZ have a low hydraulic conductivity (Sørbotten, 2011), lack horizontal differentiation (no distinct O-horizon) and have high groundwater levels. The vegetation in the GDZ consists of sparse shrubs and grasses while trees taller than 2 m are absent. Clay mineralogy on HS and in GDZ is dominated by kaolinite. A recent study (Sørbotten, 2011) showed that considerable interflow occurs along HS during rainfall episodes. Excess water moves laterally down slope in surface horizons overlaying the argic B-horizon, which has a low hydrological conductivity, thus draining the O/A- and AB-horizons on the HS relatively quickly. Discharge of interflow into GDZ results in episodically high groundwater levels and periodic waterlogging during summer (Sørbotten, 2011). Major soil characteristics for both locations are summarized in Table 1.

2.2 N₂O flux measurements

N₂O emissions were measured manually by closed chamber technique along two transects in the sub-catchment. Transect (*T*) was established perpendicular to the contour lines on the HS stretching from the hilltop close to the watershed divide to the bottom of the hill close to the GDZ. Transect (*B*) was established in the GDZ following an elevation gradient of six hydrologically connected terraces (Fig. 1b) towards a flume, which was used to measure runoff from the sub-catchment. Six plots for N₂O emission measurements ($n = 3$) and sampling of soil and pore water were established along the *T* transect on HS (T1 to T5 and B1) and five plots along the *B* transect in GDZ (B2 to B6; Fig. 1b) with plot B1 representing the transition between HS and GDZ. Two sampling strategies were applied to explore N₂O fluxes. A first measurement campaign during summer 2009 (July to September) with frequent flux measurements explored N₂O emission dynamics in response to sudden increases in soil moisture after rainfall episodes. A more regular sampling scheme with bi-weekly measurements was applied throughout the dry-cool season (November 2009 to March 2010) and during the subsequent summer (from April to August 2010), interrupted by more intensive measurement campaigns after individual rain storms (> 20 mm). For logistic reasons, only a selection of plots (T1, T3, T5, B1, B2, B4 and B6) was monitored during the dry season. In total 38 triplicate flux measurements were conducted on plots T1, T3, T5, B1, B2, B4 and B6 and 20 on plots T2, T4, B3 and B5.

Table 1. Characteristics of top soils at individual plots on the hillslope (HS) and in the groundwater discharge zone (GDZ).

| Plot | Horizon/ layer | pH | TOC | TN | C/N | BD ^a | NH ₄ ⁺ _{ex} | NO ₃ ⁻ _{ex} | NH ₄ ⁺ _{sw} | NO ₃ ⁻ _{sw} | IDR ^b | Ex situ potential of N ₂ O loss ^b | |
|------------------|-------------------|--------------------|--------------------|-------|------|-----------------|--|--|--|--|------------------|--|--|
| | | (H ₂ O) | mg g ⁻¹ | | | | g cm ⁻³ | μg N g ⁻¹ dw soil | | mg N L ⁻¹ | | nmol N ₂ O-N g ⁻¹ dw soil h ⁻¹ | nmol NO ₃ ⁻ g ⁻¹ dw soil |
| HS | T1 | O | 3.96 | 226.1 | 8.7 | 26.1 | – | 49.6 (20.2) | 37.9 (14.7) | – | – | 8.4 | 523 |
| | | A | 3.78 | 10.7 | 0.5 | 20.4 | 0.78 (0.05) | 21.5 (8.6) | 59.6 (29.2) | 0.11 (0.05) | 15.7 (3.1) | 12.2 | 552 |
| | T2 | O | 3.74 | 354.5 | 15.7 | 22.6 | – | 81.9 (11.7) | 23.7 (39.4) | – | – | 16.7 | 2336 |
| | | A | 3.84 | 15.0 | 0.8 | 19.4 | 0.72 (0.03) | 34.4 (11.9) | 12.7 (19.2) | 0.75 (0.50) | 14.9 (4.6) | 13.3 | 1056 |
| | T3 | O | 4.07 | 220.2 | 9.9 | 22.2 | – | 85.9 (19.6) | 35.7 (25.1) | – | – | 40.4 | 1924 |
| | | A | 4.13 | 12.1 | 0.6 | 19.1 | 0.73 (0.15) | 59.6 (30.1) | 20.1 (11.2) | 0.15 (0.04) | 13.3 (2.8) | 31.4 | 1624 |
| | T4 | O | 3.74 | 326.0 | 13.4 | 24.3 | – | 89.2 (16.6) | 29.1 (14.2) | – | – | 6.4 | 460 |
| | | A | 3.76 | 14.3 | 0.7 | 20.6 | 0.47 (0.03) | 32.1 (11.6) | 13.0 (4.7) | 0.07 (0.02) | 13.5 (4.1) | 16.3 | 1556 |
| | T5 | O | 3.67 | 218.1 | 10.1 | 21.6 | – | 55.3 (19.4) | 33.6 (43.6) | – | – | 26.5 | 1706 |
| | | A | 3.75 | 6.5 | 0.4 | 17.2 | 0.76 (0.16) | 25.8 (6.7) | 17.4 (6.5) | 0.07 (0.02) | 13.4 (1.7) | 14.7 | 1394 |
| B1 | O | 3.99 | 234.9 | 11.1 | 21.1 | – | 83.0 (16.6) | 25.6 (2.9) | – | – | 40.8 | 1236 | |
| | A | 4.02 | 6.05 | 0.3 | 17.6 | 0.42 (0.07) | 23.3 (5.8) | 6.6 (2.3) | 0.17 (0.07) | 13.8 (1.5) | 11.3 | 1014 | |
| GDZ ^a | 0–20 cm | B2 | 4.46 | 14.5 | 0.9 | 15.6 | 1.57 (0.09) | 3.6 (1.3) | 6.3 (1.1) | 1.25 (1.31) | 6.2 (0.5) | 1.8 | 318 |
| | | B3 | 4.31 | 12.8 | 0.7 | 18.6 | 1.67 (0.13) | 2.8 (0.8) | 2.6 (1.5) | 0.01 (0.01) | 1.5 (0.7) | 12.3 | 494 |
| | | B4 | 4.38 | 23.1 | 1.6 | 14.5 | 0.69 (0.02) | 7.9 (1.8) | 1.6 (0.5) | 0.02 (0.01) | 5.4 (0.5) | 21.0 | 53 |
| | | B5 | 4.42 | 11.8 | 0.8 | 14.4 | 0.63 (0.08) | 2.9 (1.0) | 2.4 (0.5) | 0.02 (0.01) | 0.7 (0.4) | 20.1 | 201 |
| | | B6 | 4.80 | 40.5 | 2.8 | 14.7 | 1.01 (0.13) | 4.3 (0.4) | 0.6 (0.5) | 1.12 (0.16) | 0.2 (0.0) | 28.0 | 357 |

TOC: total organic carbon; TN: total nitrogen; C/N: ratio of TOC and TN; BD: bulk density; NH₄⁺_{ex} and NO₃⁻_{ex}: average 2M KCl-extractable NH₄⁺ and NO₃⁻; NH₄⁺_{sw} and NO₃⁻_{sw}: dissolved NH₄⁺ and NO₃⁻ in soil water and groundwater in summer 2010 (11 May–26 September 2010); IDR: instantaneous denitrification rate in anoxic soil slurries with ample NO₃⁻; ex situ potential of N₂O loss: nmol NO₃⁻ g⁻¹ dw soil denitrified before maximum N₂O reduction to N₂ was observed in anoxic soil slurries with ample supply of NO₃⁻. Data in parentheses are the standard error.

^a Data from Sørbotten (2011) obtained using 100 cm³ steel cylinders in three replicates for A-horizon for each sampling plot.

^b Data from Zhu et al. (2013a).

For flux sampling, closed, vented, zinc-coated iron chambers (30 cm diameter and 30 cm in height) (Hutchinson and Mosier, 1981) were carefully pushed approx. 2 cm into the soil. Given the loamy texture and the limited number of roots in the mostly moist surface soil, this deployment method was preferred over installing permanent chamber bases which might impair surface run off and interflow during rain storms. The chamber deployment was quality assured by checking for deviations of initial (1 min after deployment) chamber N₂O concentration from ambient (~0.34 ppmv) and using CO₂ accumulation over time (not shown) to check for leakage, both of which were regular in most of the cases. Gas samples were taken from a sampling port on top of the chambers at 1, 5, 15 and 30 min after deployment by a 20-mL plastic syringe. Samples were transferred immediately to pre-evacuated 12-mL vials, crimp-sealed with butyl septa (Chromacol, UK), resulting in an overpressure to avoid contamination due to pressure changes during shipment. Chamber temperature was recorded by inserting a handheld digital thermometer into the sampling port at beginning and end of chamber deployment. Gas samples were shipped to the Norwegian University of Life Sciences and analyzed within half a year after sampling. The vials kept overpressure during shipment and storage. The samples were analyzed by ECD-gas chromatography (Model 7890A, Agilent, Santa Clara, CA, US). Carbon dioxide (CO₂) and N₂O were separated on a 20-m wide bore (0.53 mm diameter) Poraplot Q column run at 38 °C after passing a packed Heysept column used for backflushing water. Helium (He 5.0) was used as

carrier gas. The ECD was run at 375 °C with 17 mL min⁻¹ Ar/CH₄ (90/10 vol %) as makeup gas. N₂O emission rates (μg N m⁻² h⁻¹) were calculated based on the rate of change in N₂O concentration in the chamber, the internal volume of the chamber, the covered soil surface area and the average chamber temperature during deployment. For determining the rate of change in N₂O concentration in the chamber, which is the slope of a linear or a second-order polynomial fit of the concentration data against time, the R-square of both regressions were compared. Cumulative N₂O emissions for observation periods in summer 2009 (27 days, 12 July to 8 August) and summer 2010 (106 days, 10 May to 24 August) were calculated assuming a constant flux rate between sampling dates. For the calculation of cumulative N₂O emissions, only the periods with sampling frequency high enough to obtain the cumulative N₂O emission rates of the whole summer based on measurements were used.

2.3 Soil sampling and analysis

Composite soil samples were taken on 15 October 2009 from the eleven plots used for N₂O flux measurements, and analyzed for pH, total organic carbon (TOC) and total nitrogen (TN). Samples at plots T1 to T5 and B1 were taken from the O- (0–2 cm), A- (2–8 cm), AB- (8–20 cm) and B- (20–40 cm) horizons. In GDZ (plots B2 to B6), where an organic horizon was absent, the homogeneous 0–20 cm and 20–40 layers were sampled. Denitrification characteristics of the soils, investigated in a laboratory study, are reported elsewhere

(Zhu et al., 2013a). Briefly, the instantaneous denitrification rate (expressed in nmol N₂O-N g⁻¹ dw soil h⁻¹) in soils from the different plots was estimated from the N₂O accumulation rate in acetylene-treated, anoxic soil slurries at 20°C in the presence of ample NO₃⁻-N (2 mM). The soils' ex situ potential for N₂O loss (in nmol NO₃⁻-N g⁻¹ dw soil) was estimated as the amount of NO₃⁻-N respired to N₂O before N₂O reductase activity was fully expressed and rapid N₂O reduction to N₂ occurred. Since instantaneous denitrification rates were low in the deeper horizons, only data from the O- and A-horizons of HS and the 0–20 cm layer of GDZ are presented here.

Soil pH (H₂O) was measured in a suspension of 10 g dry weight (dw) soil in 50 mL deionized water with an Orion SA720 electrode pH-meter connected to an Orion ROSS Ultra pH Electrode. The contents of TOC and TN in the soil were measured in the fine earth fraction (< 2 mm), obtained after drying at 105 °C and sieving, using an element analyser (Vario EL III, Elementar Analysensysteme GmbH, Germany) at the Research Center of Eco-environmental Science, Chinese Academy of Science (RCEES, CAS). In addition, soil samples from the horizons and layers of all plots were collected three times (15 October 2009, 22 January 2010 and 29 April 2010) to measure KCl-extractable nitrate (NO₃⁻_{ex}) and ammonium (NH₄⁺_{ex}). After being sampled, soils were stored in a freezer and extracted within one month, except the soil taken on 22 January 2010, which was extracted together with the samples taken on 29 April 2010. Soil samples were extracted by shaking 10 g dw equivalents of fresh soil with 50 mL of 2M KCl for 1 h. The concentrations of NO₃⁻ and NH₄⁺ in the filtered extract were determined using Flow Injection Analysis (San⁺⁺, Skalar, the Netherlands) at RCEES, CAS.

Ceramic suction cup lysimeters (P80; Staatliche Porzellanmanufaktur, Berlin) and Macrorrhizon soil moisture sampler (Rhizosphere Research Products, The Netherlands) were installed at each plot on HS and GDZ, respectively. On the HS, lysimeters were installed in triplicate in the A- (4–5 cm), the top of the AB- (10 cm), the bottom of the AB- (20 cm) and in the B-horizon (40 cm). In the GDZ, one Macrorrhizon was installed at each of three depths (30, 60 and 100 cm). Soil water from HS was sampled from 11 November 2009, while groundwater in the GDZ was sampled from 5 August 2009; both soil water and groundwater were sampled at weekly intervals until spring 2010 and on each N₂O flux measurement date in summer 2010. Soil water from triplicate lysimeters per soil depth on HS was pooled prior to analysis. Concentrations of NO₃⁻ and NH₄⁺ in lysimeter water were measured in each sample during wet-hot seasons and in pooled samples (four weeks) during the dry-cool season, using ion chromatography (DX-120 for NH₄⁺ and DX-500 for NO₃⁻, DIONEX, USA) at the Chongqing Academy of Environmental Sciences and Monitoring, China.

Soil bulk density (BD) of surface horizons/layers was measured from intact soil cores (100cc steel cylinders) sampled in triplicate at two depths (3.5–7.2 cm and 10–13.7 cm), corresponding to the A- and AB-horizons, respectively (Sørbotten, 2011).

Soil temperature (ST) and volumetric moisture (VM, cm³ cm⁻³) at 10-cm depth were recorded every 10 min by TDR probes (Hydra Probe II) installed at plots T3 and B1 on 11 October 2009 and stored by a data logger (Campbell CR200). Data were obtained until 4 May 2011, with a malfunctioning period from 25 December 2010 to 8 February 2011. Soil water-filled pore space (WFPS) was calculated using bulk density (BD) at a depth of 10.0–13.7 cm, assuming a soil particle density (PD) of 2.65 g cm⁻³ (Linn and Doran, 1984) as

$$\text{WFPS (\%)} = \frac{\text{VM}}{1 - \frac{\text{BD}}{\text{PD}}} \times 100. \quad (1)$$

Groundwater level was monitored in PVC tubes, with a 30-cm nylon filter at the lower end, and installed at each plot along the B-transect in GDZ (B1 to B6). The PVC tubes were covered with a perforated lid to prevent pressure differences with the atmosphere. Groundwater level was measured daily from July 2009 to the beginning of August 2009 during a period of heavy rainstorms and on dates of N₂O measurements thereafter.

Meteorological data (air temperature (AT), precipitation (precip) and relative humidity (RH)) were obtained every 5 min from a weather station (WeatherHawk 232, USA), at the roof of the TSP Forest Bureau situated 1 km south of the catchment. Vapor pressure deficit (VPD, kPa) was calculated from equation 2 (ASCE, 2005) as

$$\text{VPD} = \left(\frac{\text{RH}}{100} - 1 \right) \cdot 0.6108 \cdot \exp(17.27 \cdot \text{AT}/(\text{AT} + 237.3)) \quad (2)$$

2.4 Statistical analysis

Cumulative N₂O emissions for each of the eleven plots for summer 2010 (106 days) were analyzed together with soil parameters in the top soil (depth-weighted for O and A horizons on HS and from 0–20 cm in GDZ; Table 1) by Principal Component Analysis (PCA). Bulk density, cumulative N₂O flux, NH₄⁺_{sw} and NO₃⁻_{sw} were normalized using minus reciprocal, natural logarithmic, natural logarithmic and sinusoidal transformation, respectively.

To explore the seasonal drivers of the N₂O emission flux, log-transformed average N₂O emission rates on HS (average of 4 plots, T1, T3, T5 and B1, which had full N₂O flux datasets including the dry season) were subjected to stepwise multiple linear regression with ST, WFPS (average of daily ST and WFPS obtained from TDR probes at both T3 and B1 from 12 October 2009 onwards), as well as pore water NO₃⁻_{sw} and NH₄⁺_{sw} concentration in these four plots as independent variables. The resulting empirical relation was

used to interpolate the N₂O flux on HS between measurement dates on the basis of continuously measured ST and WFPS and to estimate the annual N₂O emission of two complete annual periods: one from 5 May 2009 to 4 May 2010 and the other one from 5 May 2010 to 4 May 2011.

Missing values for ST and WFPS (from 1 May to 11 October 2009 and from 25 December 2010 to 8 February 2011) were estimated on a daily basis, using a statistical model based on multiple linear regression, using available meteorological data (average air temperature, rainfall and average VPD). General linear model (GLM) with the mixed-effects (sampling dates and location) was used for the comparison of different plots, the two landscape elements and different seasons.

All statistical analyses were conducted with Minitab 16.1.1 (Minitab Inc.).

3 Results

3.1 Weather, soil moisture and soil temperature

Rainfall distribution during the wet season (April to October) differed between the two years (Fig. 2). Summer 2009 (1054 mm) was wetter than summer 2010 (850 mm) and precipitation occurred mostly as intensive rainstorms (up to 385 mm during 41 h between 3 and 5 August 2009). In contrast, precipitation was more evenly distributed in summer 2010. Only 117 mm rain fell in the dry-cool season from November 2009 to March 2010. Soil WFPS at 10-cm depth on the mid slope (T3, mean WFPS 55.8 %) was significantly smaller than at the foot slope of HS at the transition to GDZ (B1, mean WFPS 70.0 %) (Fig. 3a), most likely reflecting convergence of interflow from HS at B1. In winter, WFPS was relatively stable with values around 56.7 % for T3 and 68.5 % for B1. In contrast, large variations in WFPS were observed in spring and summer, driven by precipitation, and subsequent drainage and evapotranspiration. In plot T3 (HS), but not in plot B1 (transition to GDZ), WFPS decreased significantly in late summer 2010 (July through September), indicating drier conditions on the upper part of HS as described earlier for this site (Mulder et al., 2005). ST at 10-cm depth varied seasonally between 10 °C and 25 °C with no significant difference between T3 and B1, although the drier T3 plot tended to have somewhat higher soil temperatures during the wet season (Fig. 3b).

The groundwater level in GDZ varied between +15 cm (above surface) and < -100 cm (below surface), with highest values at B5 and lowest at B1 (Fig. 4). The heavy rainstorm between 3 and 5 August 2009 resulted in a rapid increase of the groundwater level. The groundwater level reached its lowest values from late summer onwards, but increased in early spring, due to increased precipitation in March and April 2010. In general, the groundwater level was deepest at B1 and increased to near-surface in the order

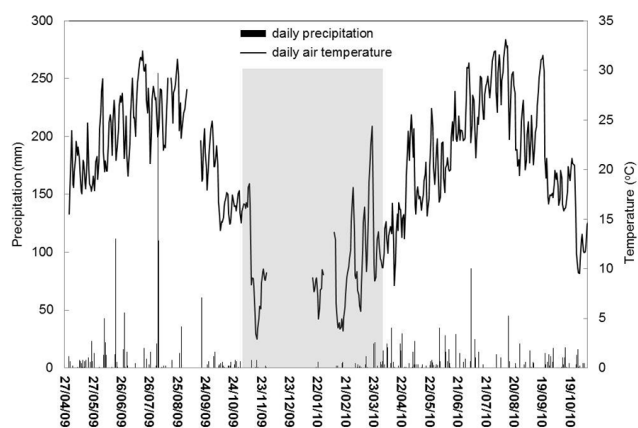


Fig. 2. Daily average air temperature and daily precipitation at TSP. The temperature data from 5 September to 18 September 2009, 29 November 2009 to 16 January 2010 and 29 January to 8 February 2010 were missing. Shaded area indicates the dry-cool season.

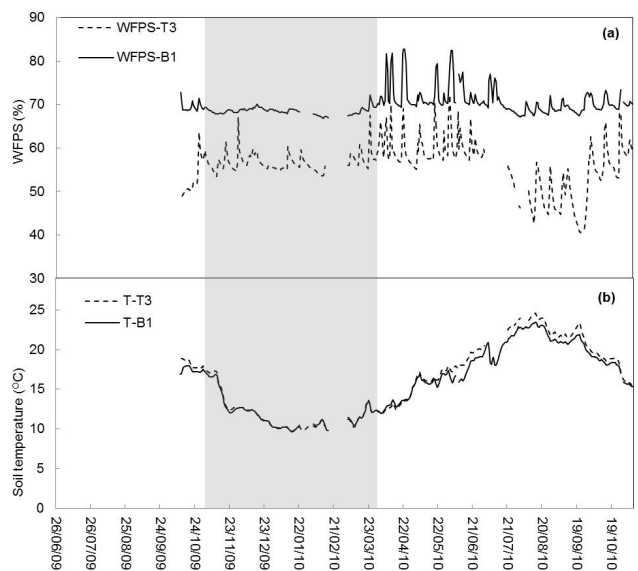


Fig. 3. (a) Soil water-filled pore space (WFPS) and (b) soil temperature (ST) at 10-cm depth at plots T3 and B1. Shaded area indicates the dry-cool season.

B1 < B2 = B3 = B4 < B5 ≤ B6 and was most stable close to the outlet (plots B5 and B6). The groundwater level was only occasionally detectable (> -100-cm depth) at plots B1, B2 and B3 (Fig. 4).

3.2 N₂O fluxes

Emission fluxes of N₂O showed a pronounced seasonal pattern with highest values during summer (wet-hot season) and significantly lower emission rates during winter (dry-cool season) ($p = 0.000$, Fig. 5). During summer, N₂O emission rates varied 1–2 orders of magnitude, with highest values

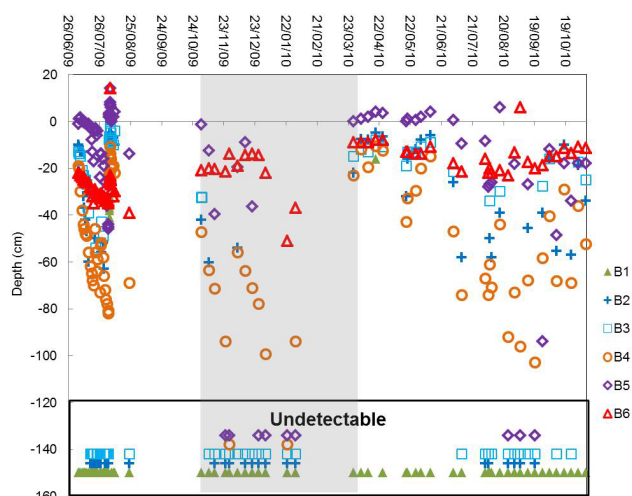


Fig. 4. Groundwater level (GWL) in GDZ. The lower panel indicates plots and dates at which the groundwater level was below the bottom of the monitoring well. Shaded area indicates the dry-cool season.

immediately following precipitation events (compare Figs. 2 and 5) when WFPS was high (Fig. 3a). In summer 2010, with its more even distribution of rainfall, peak N₂O emissions were smaller (up to 450 $\mu\text{g m}^{-2} \text{h}^{-1}$) than in summer 2009 (up to 1730 $\mu\text{g N m}^{-2} \text{h}^{-1}$) (Fig. 5). The analysis with a general linear model (GLM) indicated that N₂O emission rates were significantly higher on HS than in GDZ ($p = 0.011$). The daily average N₂O emission on HS was higher in summer 2009 (6.4 $\text{mg N m}^{-2} \text{d}^{-1}$) than in summer 2010 (3.2 $\text{mg N m}^{-2} \text{d}^{-1}$; Fig. 6). Furthermore, the average N₂O emission was smaller in GDZ than on HS, emitting on average 3.2 $\text{mg N}_2\text{O-N m}^{-2} \text{d}^{-1}$ and 1.8 $\text{mg N}_2\text{O-N m}^{-2} \text{d}^{-1}$ in 2009 and 2010, respectively. The spatial variability within the plots was high particularly on HS (Fig. 6) and no significant differences in N₂O emissions were found between plots within the same landscape element. The spatial pattern of the cumulative N₂O emissions for the plots within one transect was not consistent for the two summer periods (Fig. 6).

3.3 Spatial variability in soil factors controlling N₂O emissions

Surface soil had a greater bulk density in GDZ than on HS (Table 1) even though there were exceptions (plots B4 and B5). The pH of the surface soil was significantly higher in GDZ than on HS (Table 1). For TOC, TN and C/N the opposite was the case, reflecting the lack of an organic surface layer in GDZ. Values for the concentration of NO₃⁻ in soil extracts (NO₃⁻_{ex}) and the concentration of NO₃⁻ in soil water (NO₃⁻_{sw}) were significantly higher on HS than in GDZ. In the O-horizon, TOC and TN were higher at T2 and T4 than at other plots on HS. In the GDZ, Plot B6 was high-

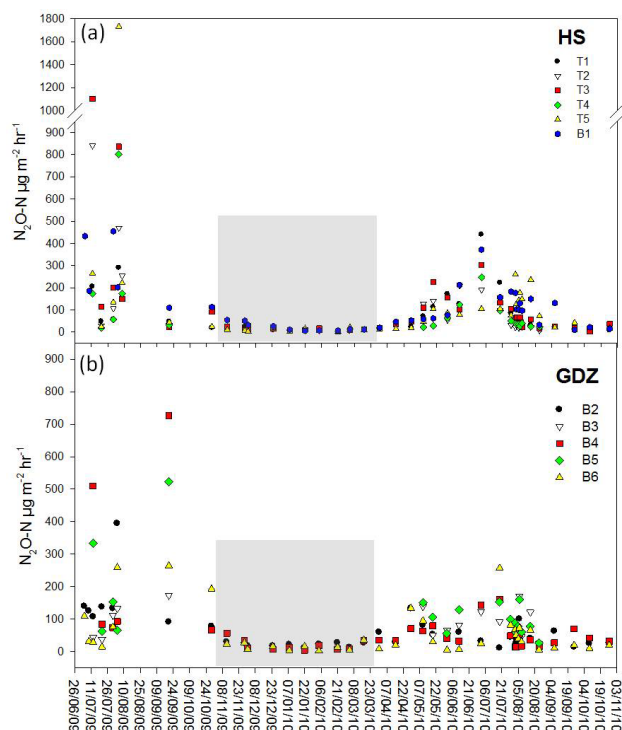


Fig. 5. (a) Mean N₂O flux ($n = 3$) at the plots on the hillslope (HS) and (b) in the groundwater discharge zone (GDZ). Standard errors are not shown to maintain readability of the figure. Shaded area indicates the dry-cool season.

est with respect to these variables. The NO₃⁻_{sw} was high in winter and early spring and decreased sharply at the start of the growing season in early April, probably due to biological uptake of N and dilution by ample rainfall at the end of March 2010 (Fig. 7). During winter, NO₃⁻_{sw} showed consistent differences among plots on HS with highest values at plot T1 and lowest at plot T2, whereas concentrations were lower and more uniform throughout summer, fluctuating with precipitation events. There were consistent differences in NO₃⁻_{sw} in GDZ, with concentration levels decreasing in the order B2 = B4 > B3 > B5 ≥ B6. At B3, B5 and B6, NO₃⁻_{sw} concentrations were below 5 mg N L^{-1} during most of the year with the greatest values at the end of the dry season (February and March 2010). The concentration of NH₄⁺ in soil water (NH₄⁺_{sw}) was small, with values amounting to less than 10 % of total inorganic N in solution, except for plots B2 and B6, and there was no seasonal pattern in any of the plots (data not shown). No correlation was found between NH₄⁺_{sw} and NO₃⁻_{sw} in soil water.

We used PCA to assess the relationship between soil parameters and the cumulative N₂O flux in summer 2010 (Fig. 6) at each plot (Fig. 8). The PCA divided the plots into two groups (T1 to T5 and B1 as one group (HS); the others as the second group (GDZ)). The first two components of PCA explained 63.9 % of the total variation, with most

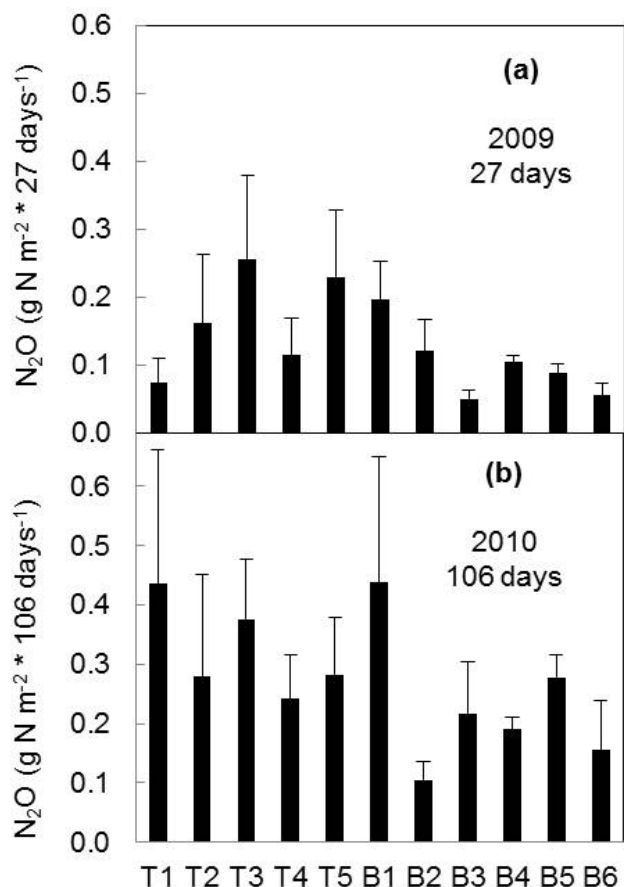


Fig. 6. ((a) Cumulative N₂O fluxes (g N₂O-N m⁻²) during summer 2009, from 12 July to 8 August, 27 days) and ((b) 2010, from 10 May to 24 August, 106 days) at individual plots ($n=3$). Error bars represent standard error.

of the physicochemical parameters (pH, bulk density, TOC, TN, NO₃⁻_{ex}, NO₃⁻_{sw} and NH₄⁺_{ex}) and the ex situ potential for N₂O loss contributing to the first component (50.3 %). The second component (13.6 %) included NH₄⁺_{sw}. The instantaneous denitrification rate contributed to both components, but had relatively small effect on the N₂O flux compared to other parameters. Total organic carbon (TOC) and most of the variables associated with the availability of N (TN, NO₃⁻_{ex}, NO₃⁻_{sw} and NH₄⁺_{ex}) were positively correlated with soil N₂O flux, whereas soil pH and bulk density (BD) were negatively correlated with N₂O flux. Also, the instantaneous denitrification rate and the ex situ potential for N₂O loss were positively correlated with N₂O flux, whereas NH₄⁺_{sw} concentration in soil water did not correlate with N₂O flux.

3.4 Temporal variability of seasonal drivers for N₂O emission

In summer, peak N₂O emission was associated with rainfall resulting in high WFPS values. Emission of N₂O on HS

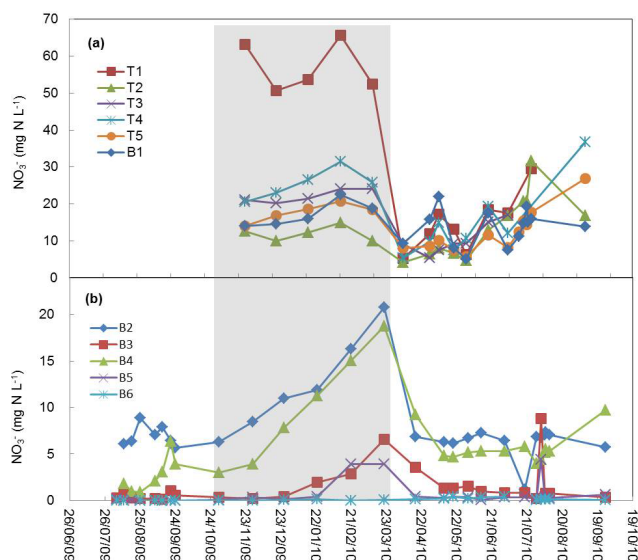


Fig. 7. (a) NO₃⁻ concentration (mg N L⁻¹) in soil pore water at 5-cm depth at each plot of HS and (b) of groundwater at 30-cm depth in GDZ. NO₃⁻ values from some of the HS plots during summer 2009 are missing because samplers were damaged by worms. Shaded area indicates the dry-cool season.

was highest at WFPS values between 63 % and 72 % (averages at 10 cm soil depth for T3 and B1, respectively) and appeared somewhat lower at values larger than 75 % (Figs. 3a and 5). Figure 5 illustrates the large interannual variability of N₂O flux between a wet year with intensive rainfall episodes (2009) and a relatively dry year (2010) with only one episode with precipitation > 50 mm day⁻¹ (82 mm in 9 h on 5 July 2010). The N₂O flux on HS was weakly, but negatively correlated with NO₃⁻_{sw} ($p=0.064$), whereas no correlation was found with NH₄⁺_{sw} ($p=0.659$). At individual sites in GDZ, the N₂O flux was weakly, but negatively correlated with the groundwater level, i.e. higher N₂O flux occurred when the groundwater level was low. Low ST together with low WFPS seemed to be the main constraints for N₂O emission activity in winter (Figs. 3 and 5). Stepwise multiple linear regression indicated that ST and WFPS were the only significant variables explaining temporal variability of N₂O emissions (Eq. 3) on HS; NO₃⁻_{sw} and NH₄⁺_{sw} concentrations did not add significantly and were excluded by the regression. The residuals of the simulated values were normally distributed (not shown), suggesting unbiased fitting of the equation (standard errors of the coefficients in parenthesis):

$$\ln(N_2O_{HS}) = -4.80(\pm 1.24) + 0.088(\pm 0.018) \text{ WFPS} + 0.178(\pm 0.024) \text{ ST}. \quad (3)$$

Adjusted coefficient of determination:

$$(R - Sq(\text{adj})) = 68.9\%$$

Since no data for ST and WFPS were available before 11 October 2009 and from 25 December 2010 to

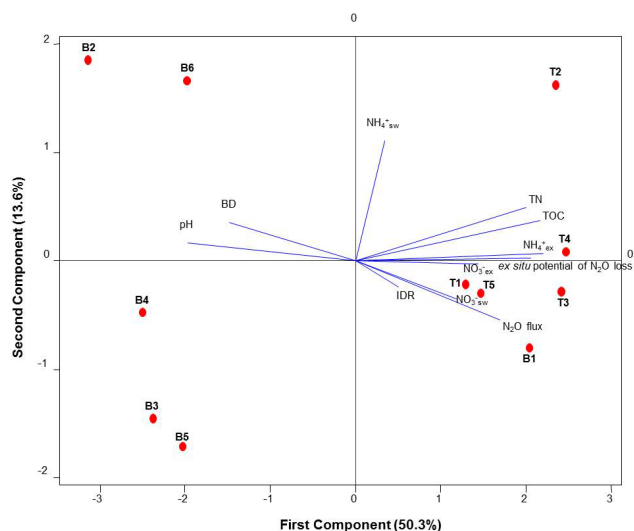


Fig. 8. Principal component analysis of cumulative N₂O fluxes and soil parameters (Table 1) at TSP. Before analysis, the N₂O flux and several of the parameters were transformed, whereas others (TOC: total organic carbon; TN: total nitrogen; C/N: the ratio of TOC and TN; IDR: instantaneous denitrification rate; ex situ potential of N₂O loss (see text for explanation); NH₄⁺_{ex} and NO₃⁻_{ex}: 2M KCl -extractable NH₄⁺ and NO₃⁻) were not. The transformations were as follows: N₂O flux: ln(cumulative N₂O flux from each plot in summer 2010; Fig. 6); bulk density (BD): $-1/(\text{bulk density})$; NH₄⁺_{sw}: ln(dissolved NH₄⁺) in soil water; NO₃⁻_{sw}: sin(dissolved NO₃⁻ in soil water). Red points indicate the individual plots.

8 February 2011, we used multiple linear regression to derive equations that link ST and WFPS to meteorological data. The resulting regression models, presented in Eqs. (4) and (5) were then used to estimate the missing values (standard errors of the coefficients in parenthesis):

$$\text{ST} = 7.84(\pm 0.41) + 0.579(\pm 0.029) \text{AT} + 1.20(\pm 0.187) \text{VPD}. \quad (4)$$

Adjusted coefficient of determination:
($R - Sq(\text{adj})$) = 67.4 %.

$$\text{WFPS} = 63.2(\pm 0.27) + 0.209(\pm 0.014) \text{precip}_5 + 1.84(\pm 0.17) \text{VPD}_5 \quad (5)$$

Adjusted coefficient of determination:
($R - Sq(\text{adj})$) = 58.8 %.

Where precip_5 (mm) is the day-weighted 5-day average precipitation prior to the date for which the computation was done (calculated as $1.0 \cdot \text{precip}_{\text{day}(0)} + 0.8 \cdot \text{precip}_{\text{day}(-1)} + 0.6 \cdot \text{precip}_{\text{day}(-2)} + 0.4 \cdot \text{precip}_{\text{day}(-3)} + 0.2 \cdot \text{precip}_{\text{day}(-4)}$) and VPD_5 (kPa) the day-weighted 5-day average vapor pressure deficit calculated analogously. The selected weights fitted the observations best. The residuals of the model simulations were normally distributed (not shown). Equation (3) was

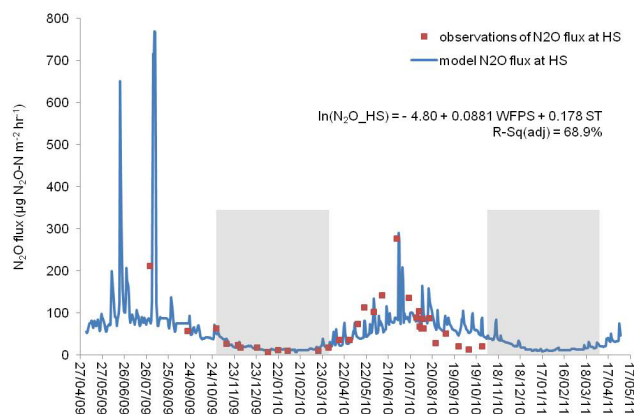


Fig. 9. Observed and simulated average N₂O flux at hillslope (HS). The shaded area denotes the dry-cool season.

used to estimate N₂O emissions using measured and simulated values for ST (Eq. 4) and WFPS (Eq. 5). Measured and simulated values are shown in Fig. 9.

3.5 Annual N₂O flux

Annual N₂O emissions on the HS were calculated at a daily time step from equation 3 for two 1-yr periods (5 May 2009 to 4 May 2010 and 5 May 2010 to 4 May 2011) (Fig. 9). The first annual period included a relatively wet summer, whereas the second period had a relatively dry summer. Annual N₂O fluxes for HS were 0.54 and 0.43 g N m⁻² for the two years, respectively, about 24 % higher in the first year than in the second. Higher annual N₂O emission in the first year may be attributed to the contribution of the frequent rain episodes in the wet summer of 2009. The N₂O emission occurring during the first 5 days after the largest rainfall episode (4 to 5 August 2009) contributed 15.8 % to the annual N₂O emission. Emissions during the dry-cool season in the first year (November 2009 to March 2010) contributed 12.0 % to the annual flux of N₂O. Also the emissions during the dry-cool season in the second year (November 2010 to March 2011), solely based on model estimates, was found to be low, contributing 16.9 % to the annual flux of N₂O.

4 Discussion

N₂O emission rates recorded after the heavy rainstorm in 2009 (up to 1730 µg N₂O-N m⁻² h⁻¹; Fig. 5) are the highest found for forest ecosystems so far and exceed rates reported for (sub)tropical forests which typically vary between 11 to 600 µg N₂O-N m⁻² h⁻¹ (Liu et al., 2011a; Zhang et al., 2008; Silver et al., 2005; Ishizuka et al., 2005; Koehler et al., 2009; Rowlings et al., 2012; Kiese and Butterbach-Bahl, 2002).

Temporal variability (Fig. 5) exceeded spatial variability in both landscape elements (HS and GDZ). However, small-scale (within-plot) variability of the cumulative N₂O flux over the active season was high as seen from the high

standard errors in Fig. 6 (particularly for HS). It is likely that this small scale variability was blurring existing trends in flux strength between plots along the HS. Large small-scale spatial variability of N₂O emissions is often reported for forest soils (Robertson and Klemmedtsson, 1996; Bowden et al., 1992; Werner et al., 2007b) and is commonly attributed to small-scale variation in mineral N availability, litter quality and soil moisture. We arranged the plots along transects perpendicular to the contour lines in the two landscape units because gradients in WFPS on HS and in groundwater level in GDZ might affect N₂O emissions by controlling aeration, substrate level and ultimately microbial activity (Garten et al., 1994). However, we did not find any consistent relationship between cumulative N₂O emission and plot position in either of the two landscape elements. Concentrations of NO₃⁻_{sw} on HS were similar at all plots during the wet-hot season (Fig. 7a) and did not correlate with N₂O emissions. The availability of NO₃⁻ was higher than in other studies (e.g., Koehler et al., 2009; Zhang et al., 2008) and appeared to be non-limiting for N₂O production on the HS, probably explaining the lack of a directional gradient in cumulative N₂O emissions as reported by others (Nishina et al., 2009; Fang et al., 2009). Surprisingly, the clear difference in WFPS between the mid slope position T3 and the foot slope position B1 (Fig. 3a) in spring and early summer did not result in significantly different cumulative N₂O emissions (Fig. 6). This was probably due to the fact that soil moisture was measured at 10-cm depth (in the upper AB-horizon), rather than in the zone of maximum denitrification activity, located in the uppermost soil layers (O- and A-horizons; Zhu et al., 2013a). Soil moisture data records for 5-cm depth were incomplete due to sensor problems, but comparing existing data and bulk densities at 5-cm depth suggests that WFPS was more similar in the uppermost soil layer (data not shown). The pronounced decrease in WFPS at T3 (but not B1), later in summer, markedly reduced N₂O emissions as compared with B1 (insert Fig. 5).

In GDZ, decreasing NO₃⁻ concentrations along the hydrological flow path (Fig. 7b) suggested strong N retention. Both NO₃⁻ and the dissolved N₂O (data not shown) concentrations in the groundwater were found to be very low at the outlet of GDZ (B5 and B6), suggesting more complete N₂O reduction along the flow path as NO₃⁻ became depleted. There was a weak trend of decreasing cumulative N₂O emissions with increasing average groundwater level along the hydrological flow path in the GDZ (with the exception of B3) during summer 2009, when the groundwater level was very dynamic (Fig. 6a). No such pattern was seen in the hydrologically more stable summer of 2010 (Fig. 6b). In general, groundwater level fluctuations are likely to interact with NO₃⁻ in controlling N₂O emissions, as the rise of groundwater level can transport NO₃⁻ into C-richer upper soil layers and create anoxia favorable for denitrification. At the same time, the residence time of N₂O in the soil profile increases, due to decreasing diffusion, thus increasing the chance of N₂O be-

ing reduced to N₂. Conversely, a drop in groundwater level may relieve gaseous diffusion constraints leading to release of N₂O from the soil. In summer 2010 (Fig. 5), for instance, N₂O emission rates were lowest at B6 until groundwater level dropped about 10 cm in the middle of July (Fig. 4), resulting in a single N₂O emission peak while returning to low levels quickly thereafter. Similar N₂O dynamics have been observed in rice paddies (e.g. Qin et al., 2010).

We found clear differences in N₂O source strength and environmental controls when comparing HS and GDZ; average cumulative N₂O emission in GDZ was roughly half of this at HS in both summers (Figs. 5 and 6), which was surprising, as we expected GDZ to behave as a riparian zone with elevated denitrification activity. Riparian zones are commonly considered as “hot spots” for N₂O emissions, because they receive dissolved N (DON, NO₃⁻) from surrounding slopes while providing optimal conditions for denitrification (DOC, anoxia) (Groffman et al., 2000; Hefting et al., 2003). However, unlike common riparian zones which typically develop soils rich in organic matter, the GDZ studied here is formed by formerly cultivated terraces on colluvial deposits. Soils are dense and have low hydrological conductivities, resulting in low productivity and low TOC contents (Table 1). Laboratory incubations revealed that the GDZ soils had instantaneous denitrification rates similar to HS soils, despite their markedly lower TOC contents (Zhu et al., 2013a). This indicated a similar N removal potential in GDZ as compared with HS. However in their study, Zhu et al. (2013a) also found that denitrifying communities on HS and in GDZ differed functionally with respect to their product stoichiometry, with the GDZ communities being more efficient in reducing NO₃⁻ all the way to N₂. Thus, the lower N₂O/N₂ ratio, and consequently the reduced N₂O emission rate, in GDZ may be attributed to a number of site-specific factors, directly or indirectly affecting denitrifier functioning and stoichiometry: (1) pore water at GDZ had lower NO₃⁻ concentrations (Figs. 7b and 8), which may decrease the N₂O/N₂ ratio by forcing denitrifiers to utilize N₂O as an additional electron acceptor; (2) diffusion of N₂O in soil is slow in dense GDZ soils, resulting in higher dissolved N₂O concentrations in pore water (data not shown), which supports denitrifier communities to express N₂O reductase; and (3) soil pH at GDZ was 0.5–0.6 units higher than at HS, which directly (Bergaust et al., 2010) or indirectly (Liu et al., 2010a; Simek and Cooper, 2002; Dörsch et al., 2012) lowers N₂O/N₂ ratios.

Even though this study was not designed to discriminate sources of N₂O emission, several observations indicate that N₂O emission rates during the active periods were more sensitive to denitrification controls than nitrification controls: (1) on the HS, high N₂O emission occurred when soil WFPS was high; (2) in the GDZ, dissolved N₂O decreased with NO₃⁻ concentration in groundwater; (3) the difference in magnitude in N₂O flux on HS and in GDZ was congruent to differences in denitrification stoichiometry observed in soils from

the two landscape elements in laboratory incubations (Zhu et al., 2013a); (4) N₂O concentrations measured in soil air were negatively correlated with pO_2 ($R^2 = 0.40$, $p = 0.000$, data not shown). Low nitrification rates have been reported for acidic forest soils in SW China (Cai and Zhao, 2009). However, given the prevalence of NH_4^+ in deposited N and its rapid disappearance in the soil solution, NH_4^+ oxidizing processes could be a potentially important source for N₂O emission. We conducted an in situ $^{15}NO_3^-$ labeling experiment in summer 2010 at two positions along the HS reported elsewhere (Zhu et al., 2013b) and found that 71–100 % of the emitted N₂O derived from the labeled soil NO_3^- pool. It seemed that even though the fate of the deposited NH_4^+ remains unclear in this catchment, nitrification is not the main source for the high N₂O emission observed.

We found large temporal variability in N₂O fluxes. Multiple linear regression identified ST and WFPS as the main drivers, explaining 68.9 % of the temporal variability of N₂O emission fluxes on HS. Such a high coefficient of determination with only two variables is remarkable as most studies conducted in forest ecosystems report much lower degree of explanation by ancillary variables (Morishita et al., 2011; Gu et al., 2011). As shown in Fig. 9, the resulting regression model captured reasonably well both the seasonal distribution of emission fluxes and the transient emission peaks after rainfall events on HS except for the first measurement point. Peak N₂O emissions (Fig. 5) were triggered by spikes in WFPS (Fig. 3a) occurring after big rain episodes, resulting in a highly skewed distribution of N₂O fluxes as found in many other studies (Khalil et al., 2007; Venterea et al., 2009). Low ST, together with relatively low WFPS throughout winter resulted in low N₂O fluxes. This implies that N₂O emission fluxes can be estimated fairly well from discontinuous flux measurements when continuous data on ST and WFPS are available. However, it is important to sample fluxes closely around major rain fall events in summer as they contribute disproportionately to overall emissions. Overly long intervals between samplings may result in over- or underestimation of the cumulative flux (Parkin, 2008).

Annual N₂O emissions for the TSP catchment were estimated for the HS only, since 96.4 % of the area consists of hillslopes, rendering GDZ emissions a minor component of the overall N₂O budget. Annual fluxes showed considerable variation between the wet year (May 2009 to April 2010) with several intensive rain episodes ($0.54 \text{ g N}_2\text{O-N m}^{-2} \text{ yr}^{-1}$) and the dryer year (May 2010 to April 2011) with more evenly distributed precipitation ($0.43 \text{ g N}_2\text{O-N m}^{-2} \text{ yr}^{-1}$). The average annual N₂O emission flux in TSP ($0.48 \text{ g N m}^{-2} \text{ yr}^{-1}$) is at the high end of annual N₂O emission fluxes ($0.005\text{--}0.47 \text{ g N m}^{-2} \text{ yr}^{-1}$) reported for unfertilized forestland in China (Cai, 2012). The fluxes are even comparable to the high end of reported N₂O fluxes in tropical rainforests where temperatures are high throughout the year (Dalal and Allen, 2008) and to a tropical lowland for-

est in Panama which was experimentally N-enriched for 9–10 years (Koehler et al., 2009). Expressed as a fraction of the annual atmo-genic N-deposition, N₂O-N emission amounted to between 8 and 10 % of the incoming inorganic N. This “emission factor” was much higher than the Tier 1 IPCC default factor (1 %) used for accounting both direct N₂O emissions arising from mineral N fertilizer application to managed soils and indirect N₂O emissions arising from the redeposited N to uncultivated soils (IPCC, 2006). The emission factor derived from our study is at the high end of the reported N₂O emission factors for deciduous forests and coniferous forests, which were on average 6.5 % and 2.4 %, respectively (van der Gon and Bleeker, 2005). This pinpoints the prominent role of nitrogen-saturated, subtropical forests on acid soils as a secondary source of anthropogenic N₂O, which should be taken into account for regional N₂O budgets.

Acknowledgements. This study was supported by the Norwegian research council (Nordklima program 193725/S30: “N₂O emissions from N saturated subtropical forest in South China”) and the Chinese Academy of Sciences (No. KZCX2-YW-GJ01 and GJHZ1205). We are grateful for technical support by Zhang Guanli at the Chongqing Academy of Environmental Sciences, Zhang Xiaoshan at the Research Center for Eco-environmental Sciences, Chinese Academy of Sciences and T. Fredriksen at the Norwegian University of Life Sciences. We also thank Duan Lei at the Tsinghua University for providing N deposition data and L. E. Sørbotten and J. Stolte (both Bioforsk, Norway) for data on soil hydrology and assistance in the field.

Edited by: E. Veldkamp

References

- Aber, J. D., Goodale, C. L., Ollinger, S. V., Smith, M. L., Magill, A. H., Martin, M. E., Hallett, R. A., and Stoddard, J. L.: Is nitrogen deposition altering the nitrogen status of northeastern forests?, *Bioscience*, 53, 375–389, 2003.
- ASCE, S. o. R. E. T. C. o.: The ASCE standardized reference evapotranspiration equation, environmental and water resources, Institute of the American Society of Civil Engineers, 2005.
- Banerjee, S. and Siciliano, S. D.: Factors driving potential ammonia oxidation in Canadian arctic ecosystems: does spatial scale matter?, *Appl. Environ. Microb.*, 78, 346–353, 2012.
- Bergaust, L., Mao, Y. J., Bakken, L. R., and Frostegard, A.: Denitrification response patterns during the transition to anoxic respiration and posttranscriptional effects of suboptimal pH on nitrogen oxide reductase in *Paracoccus denitrificans*, *Appl. Environ. Microb.*, 76, 6387–6396, 2010.
- Bowden, W. B., McDowell, W. H., Asbury, C. E., and Finley, A. M.: Riparian nitrogen dynamics in 2-geomorphologically distinct tropical rain-forest watersheds – nitrous-oxide fluxes, *Biogeochemistry*, 18, 77–99, 1992.
- Cai, Z. C.: Greenhouse gas budget for terrestrial ecosystems in China, *Sci. China-Earth Sci.*, 55, 173–182, 2012.
- Cai, Z. C. and Zhao, W.: Effects of land use types on nitrification in humid subtropical soils of China, *Acta Pedologica Sinica*, 46, 7, 2009 (in Chinese).

- Chen, X. Y. and Mulder, J.: Indicators for nitrogen status and leaching in subtropical forest ecosystems, South China, *Biogeochemistry*, 82, 165–180, 2007a.
- Chen, X. Y. and Mulder, J.: Atmospheric deposition of nitrogen at five subtropical forested sites in South China, *Sci. Total Environ.*, 378, 317–330, 2007b.
- D'Amelio, M. T. S., Gatti, L. V., Miller, J. B., and Tans, P.: Regional N₂O fluxes in Amazonia derived from aircraft vertical profiles, *Atmos. Chem. Phys.*, 9, 8785–8797, doi:10.5194/acp-9-8785-2009, 2009.
- Dalal, R. C. and Allen, D. E.: Greenhouse gas fluxes from natural ecosystems, *Aust. J. Bot.*, 56, 369–407, 2008.
- De Boer, W. and Kowalchuk G. A.: Nitrification in acid soils: microorganisms and mechanisms, *Soil Biol. Biochem.*, 33, 853–866, 2001.
- Dörsch, P., Braker, G., and Bakken, L. R.: Community specific pH response of denitrification: experiments with cells extracted from organic soils, *FEMS Microbiol. Ecol.*, 79, 530–541, 2012.
- Fang, Y. T., Gundersen, P., Zhang, W., Zhou, G. Y., Christiansen, J. R., Mo, J. M., Dong, S. F., and Zhang, T.: Soil-atmosphere exchange of N₂O, CO₂ and CH₄ along a slope of an evergreen broad-leaved forest in southern China, *Plant Soil*, 319, 37–48, 2009.
- Flessa, H., Dörsch, P., and Beese, F.: Seasonal-variation of N₂O and CH₄ fluxes in Differently managed arable soils in southern Germany, *J. Geophys. Res.-Atmos.*, 100, 23115–23124, 1995.
- Garten, C. T., Huston, M. A., and Thoms, C. A.: Topographic variation of soil-nitrogen dynamics at Walker Branch watershed, Tennessee, *Forest Sci.*, 40, 497–512, 1994.
- Groffman, P. M., Gold, A. J., and Addy, K.: Nitrous oxide production in riparian zones and its importance to national emission inventories, *Chemosphere*, 2, 291–299, 2000.
- Gu, J. X., Nicoulaud, B., Rochette, P., Pennock, D. J., Henault, C., Cellier, P., and Richard, G.: Effect of topography on nitrous oxide emissions from winter wheat fields in Central France, *Environ. Pollut.*, 159, 3149–3155, 2011.
- Hefting, M. M., Bobbink, R., and de Caluwe, H.: Nitrous oxide emission and denitrification in chronically nitrate-loaded riparian buffer zones, *J. Environ. Qual.*, 32, 1194–1203, 2003.
- Hirsch, A. I., Michalak, A. M., Bruhwiler, L. M., Peters, W., Dlugokencky, E. J., and Tans, P. P.: Inverse modeling estimates of the global nitrous oxide surface flux from 1998–2001, *Global Biogeochem. Cy.*, 20, Gb1008, doi:10.1029/2004gb002443, 2006.
- Hutchinson, G. L. and Mosier, A. R.: Improved soil cover method for field measurement of nitrous oxide fluxes, *Soil Sci. Soc. Am. J.*, 45, 311–316, 1981.
- IPCC (2007) Summary for policy makers, in: *Climate Change 2007: The physical Science Basis, Contribution of Working Group I to the Fourth Assessment Report of the Intergovernmental Panel on Climate Change*, edited by: Solomon, S., Qin, D., Manning, M., Chen, Z., Marquis, M., Averyt, K. B., Tignor, M., and Miller, H. L., Cambridge, UK and New York, USA, 2007.
- IPCC (2006) Agriculture, Forestry and Other Land Use, in: *Guidelines for National Greenhouse Gas Inventories*, edited by: Eggleston, H. S., Buendia, L., Miwa, K., Ngara, T., and Tanabe, K., IGES, Japan, 2006.
- Ishizuka, S., Iswandi, A., Nakajima, Y., Yonemura, L., Sudo, S., Tsuruta, H., and Muriyarso, D.: Spatial patterns of greenhouse gas emission in a tropical rainforest in Indonesia, *Nutr. Cycl. Agroecosys.*, 71, 55–62, 2005.
- Khalil, M. I., Van Cleemput, O., Rosenani, A. B., and Schmidhalter, U.: Daytime, temporal, and seasonal variations of N₂O emissions in an upland cropping system of the humid tropics, *Commun. Soil Sci. Plan.*, 38, 189–204, 2007.
- Kiese, R. and Butterbach-Bahl, K.: N₂O and CO₂ emissions from three different tropical forest sites in the wet tropics of Queensland, Australia, *Soil Biol. Biochem.*, 34, 975–987, 2002.
- Koehler, B., Corre, M. D., Veldkamp, E., Wullaert, H., and Wright, S. J.: Immediate and long-term nitrogen oxide emissions from tropical forest soils exposed to elevated nitrogen input, *Global Change Biol.*, 15, 2049–2066, 2009.
- Kort, E. A., Patra, P. K., Ishijima, K., Daube, B. C., Jimenez, R., Elkins, J., Hurst, D., Moore, F. L., Sweeney, C., and Wofsy, S. C.: Tropospheric distribution and variability of N₂O: Evidence for strong tropical emissions, *Geophys. Res. Lett.*, 38, L15806, doi:10.1029/2011gl047612, 2011.
- Lark, R. M., Milne, A. E., Addiscott, T. M., Goulding, K. W. T., Webster, C. P., and O'Flaherty, S.: Scale- and location-dependent correlation of nitrous oxide emissions with soil properties: an analysis using wavelets, *Eur. J. Soil Sci.*, 55, 611–627, 2004.
- Larsen, T., Duan, L., and Muder, J.: Deposition and leaching of sulfur, nitrogen and calcium in four forested catchments in China: implications for acidification, *Environ. Sci. Technol.*, 45, 1192–1198, 2011.
- Lin, S., Iqbal, J., Hu, R. G., and Feng, M. L.: N₂O emissions from different land uses in mid-subtropical China, *Agr. Ecosyst. Environ.*, 136, 40–48, 2010.
- Lin, S., Iqbal, J., Hu, R. G., Ruan, L. L., Wu, J. S., Zhao, J. S., and Wang, P. J.: Differences in nitrous oxide fluxes from red soil under different land uses in mid-subtropical China, *Agr. Ecosyst. Environ.*, 146, 168–178, 2012.
- Linn D. M. and Doran J. W.: Effect of water-filled pore-space on carbon dioxide and nitrous oxide production in tilled and non-tilled soils, *Soil Sci. Soc. Am. J.*, 48, 1267–1272, 1984.
- Liu, B. B., Morkved, P. T., Frostegard, A., and Bakken, L. R.: Denitrification gene pools, transcription and kinetics of NO, N₂O and N₂ production as affected by soil pH, *FEMS Microbiol. Ecol.*, 72, 407–417, 2010a.
- Liu, B. B., Morkved, P. T., Frostegard, A., and Bakken, L. R.: Denitrification gene pools, transcription and kinetics of NO, N₂O and N₂ production as affected by soil pH, *FEMS Microbiol. Ecol.*, 72, 407–417, 2010b.
- Liu, J., Jiang, P. K., Li, Y. F., Zhou, G. M., Wu, J. S., and Yang, F.: Responses of N₂O Flux from Forest Soils to Land Use Change in Subtropical China, *Bot. Rev.*, 77, 320–325, 2011a.
- Liu, X. J., Duan, L., Mo, J. M., Du, E. Z., Shen, J. L., Lu, X. K., Zhang, Y., Zhou, X. B., He, C. N., and Zhang, F. S.: Nitrogen deposition and its ecological impact in China: An overview, *Environ. Pollut.*, 159, 2251–2264, 2011b.
- Melillo, J. M., Steudler, P. A., Feigl, B. J., Neill, C., Garcia, D., Piccolo, M. C., Cerri, C. C., and Tian, H.: Nitrous oxide emissions from forests and pastures of various ages in the Brazilian Amazon, *J. Geophys. Res.-Atmos.*, 106, 34179–34188, 2001.
- Morishita, T., Aizawa, S., Yoshinaga, S., and Kaneko, S.: Seasonal change in N₂O flux from forest soils in a forest catchment in Japan, *J. For. Res.*, 16, 386–393, 2011.
- Mørkved, P. T., Dörsch, P., and Bakken, L. R.: The N₂O product ratio of nitrification and its dependence on long-term changes in

- soil pH, *Soil Biol. Biochem.*, 39, 2048–2057, 2007.
- Mulder, J., Chen, X. Y., Zhao, D. W., and Xiang, R. J.: Elevated nitrogen deposition in subtropical Chinese forest ecosystems, dominated by Masson pine: Nitrogen fluxes and budgets at the plot and catchment scale, The 3rd international N conference, Nanjing, China, 12–16 October 2004, 2005.
- Nishina, K., Takenaka, C., and Ishizuka, S.: Spatiotemporal variation in N₂O flux within a slope in a Japanese cedar (*Cryptomeria japonica*) forest, *Biogeochemistry*, 96, 163–175, 2009.
- Osaka, K., Ohte, N., Koba, K., Katsuyama, M., and Nakajima, T.: Hydrologic controls on nitrous oxide production and consumption in a forested headwater catchment in central Japan, *J. Geophys. Res.-Biogeo.*, 111, G01013, doi:10.1029/2005jg000026, 2006.
- Parkin, T. B.: Effect of sampling frequency on estimates of cumulative nitrous oxide emissions, *J. Environ. Qual.*, 37, 1390–1395, 2008.
- Parton, W. J., Mosier, A. R., Ojima, D. S., Valentine, D. W., Schimel, D. S., Weier, K., and Kulmala, A. E.: Generalized model for N₂ and N₂O production from nitrification and denitrification, *Global Biogeochem. Cy.*, 10, 401–412, 1996.
- Philippot, L., Cuhel, J., Saby, N. P. A., Cheneby, D., Chronakova, A., Bru, D., Arrouays, D., Martin-Laurent, F., and Simek, M.: Mapping field-scale spatial patterns of size and activity of the denitrifier community, *Environ. Microb.*, 11, 1518–1526, 2009.
- Qin, Y. M., Liu, S. W., Guo, Y. Q., Liu, Q. H., and Zou, J. W.: Methane and nitrous oxide emissions from organic and conventional rice cropping systems in Southeast China, *Biol. Fert. Soils*, 46, 825–834, 2010.
- Raich, J. W. and Schlesinger, W. H.: The global carbon dioxide flux in soil respiration and its relationship to vegetation and climate, *Tellus B*, 44, 81–99, 1992.
- Robertson, K. and Klemmedtsson, L.: Assessment of denitrification in organogenic forest soil by regulating factors, *Plant Soil*, 178, 49–57, 1996.
- Rowlings, D. W., Grace, P. R., Kiese, R., and Weier, K. L.: Environmental factors controlling temporal and spatial variability in the soil-atmosphere exchange of CO₂, CH₄ and N₂O from an Australian subtropical rainforest, *Global Change Biol.*, 18, 726–738, 2012.
- Silver, W. L., Thompson, A. W., McGroddy, M. E., Varner, R. K., Dias, J. D., Silva, H., Crill, P. M., and Keller, M.: Fine root dynamics and trace gas fluxes in two lowland tropical forest soils, *Global Change Biol.*, 11, 290–306, 2005.
- Simek, M. and Cooper, J. E.: The influence of soil pH on denitrification: progress towards the understanding of this interaction over the last 50 years, *Eur. J. Soil Sci.*, 53, 345–354, 2002.
- Smith, K. A., Ball, T., Conen, F., Dobbie, K. E., Massheder, J., and Rey, A.: Exchange of greenhouse gases between soil and atmosphere: interactions of soil physical factors and biological processes, *Eur. J. Soil Sci.*, 54, 779–791, 2003.
- Sørbotten, L.: Hill slope unsaturated flowpaths and soil moisture variability in a forested catchment in southwest China, Master, Department of Plant and environmental sciences, Norwegian University of Life Sciences, Aas, 64 pp., 2011.
- Stehfest, E. and Bouwman, L.: N₂O and NO emission from agricultural fields and soils under natural vegetation: summarizing available measurement data and modeling of global annual emissions, *Nutr. Cycl. Agroecosys.*, 74, 207–228, 2006.
- Tang, X. L., Liu, S. G., Zhou, G. Y., Zhang, D. Q., and Zhou, C. Y.: Soil-atmospheric exchange of CO₂, CH₄, and N₂O in three subtropical forest ecosystems in southern China, *Global Change Biol.*, 12, 546–560, 2006.
- Van der Gon, H. D. and Bleeker, A.: Indirect N₂O emission due to atmospheric N deposition for the Netherlands, *Atmos. Environ.*, 39, 5827–5838, 2005.
- Venterea, R. T., Spokas, K. A., and Baker, J. M.: Accuracy and Precision Analysis of Chamber-Based Nitrous Oxide Gas Flux Estimates, *Soil Sci. Soc. Am. J.*, 73, 1087–1093, 2009.
- Weier, K. L., Doran, J. W., Power, J. F., and Walters, D. T.: Denitrification and dinitrogen nitrous-oxide ratio as affected by soil-water, available carbon and nitrate, *Soil Sci. Soc. Am. J.*, 57, 66–72, 1993.
- Werner, C., Butterbach-Bahl, K., Haas, E., Hickler, T., and Kiese, R.: A global inventory of N₂O emissions from tropical rainforest soils using a detailed biogeochemical model, *Global Biogeochem. Cy.*, 21, Gb3010 doi:10.1029/2006gb002909, 2007a.
- Werner, C., Kiese, R., and Butterbach-Bahl, K.: Soil-atmosphere exchange of N₂O, CH₄, and CO₂ and controlling environmental factors for tropical rain forest sites in western Kenya, *J. Geophys. Res.-Atmos.*, 112, doi:10.1029/2006jd007388, D03308, 2007b.
- Wessen, E., Soderstrom, M., Stenberg, M., Bru, D., Hellman, M., Welsh, A., Thomsen, F., Klemmedtson, L., Philippot, L., and Hallin, S.: Spatial distribution of ammonia-oxidizing bacteria and archaea across a 44-hectare farm related to ecosystem functioning, *ISME J.*, 5, 1213–1225, 2011.
- WMO: The state of greenhouse gases in the atmosphere using global observations through 2008, in: *Greenhouse Gas Bulletin*, World Meteorological Organization, 4, 2009.
- WRB: World reference base for soil resources, 2006, FAO, Rome, 3 b. pp., 2006.
- Xiong, Z. Q., Freney, J. R., Mosier, A. R., Zhu, Z. L., Lee, Y., and Yagi, K.: Impacts of population growth, changing food preferences and agricultural practices on the nitrogen cycle in East Asia, *Nutr. Cycl. Agroecosys.*, 80, 189–198, 2008.
- Zhang, W., Mo, J. M., Yu, G. R., Fang, Y. T., Li, D. J., Lu, X. K., and Wang, H.: Emissions of nitrous oxide from three tropical forests in Southern China in response to simulated nitrogen deposition, *Plant Soil*, 306, 221–236, 2008.
- Zhou, G. Y., Guan, L. L., Wei, X. H., Tang, X. L., Liu, S. G., Liu, J. X., Zhang, D. Q., and Yan, J. H.: Factors influencing leaf litter decomposition: an intersite decomposition experiment across China, *Plant Soil*, 311, 61–72, 2008.
- Zhu J., Mulder J., Solheimslid S., and Dörsch P.: Functional traits of denitrification in a subtropical forest catchment in China with high atrogenic N deposition, *Soil Biol. Biochem.*, 57, 577–586, 2013a.
- Zhu J., Mulder J., Bakken L., and Dörsch P.: The importance of denitrification in N₂O emission from N-saturated forests of SW China; results from in situ ¹⁵N labeling experiments, *Biogeochemistry*, in review, 2013b.